

The amidine formed by tacrine and saccharin revisited: An ab initio Investigation of Structural, Electronic and Spectroscopic Properties

Nursel ACAR SELÇUKİ¹

Ege University, Faculty of Science, Chemistry Department, 35100 Izmir / Turkey

Abstract: Computational study of tacrine and saccharin and their amidine complex (TacSac) was performed by ab initio calculations including electron correlation. Structure, UV-Vis spectra and charge distribution of the amidine (TacSac) were investigated using ground state geometries optimized at MP2/6-311++G(d,p) level. The effects of solvent was investigated using polarizable continuum model (PCM) in conjunction with the solvation model based on density (SMD) approach. TacSac geometry remained same in gas phase and in H₂O both with PCM and SMD models in contrast to former DFT results. The amidine is calculated to be stable indicating that former DFT calculations underestimated the stability of the investigated amidine. UV-Vis spectra and electronic transitions were calculated at CIS/6-311++G(d,p), B3LYP/6-311++G(d,p) and CAM-B3LYP/6-311++G(d,p) levels of theory and B3LYP gave the best results. TacSac has a peak at a higher wavelength enabling S₀→S₁ transition with a lower energy. S₀→S₁ transition corresponds to full charge transfer between HOMO and LUMO orbitals of TacSac in H₂O. The ab initio results indicate that the TacSac system can be synthesized with an easy condensation reaction, and that the amidine product is a potential candidate for photochemical charge-transfer systems.

Keywords: Amidine, Møller-Plesset, Density Functional Theory, Tacrine, Saccharin

1. Introduction

Interactions of molecules under physiological conditions are of great interest as they can be directly involved in human metabolism. Especially, drugs and nutrient components receive a special interest as they play critical roles in human daily life.

One of these compounds is tacrine (1,2,3,4-tetrahydroacridin-9-amine, Fig. 1) which was first synthesized towards the end of World War II [1]. It was among the 90 acridine derivatives obtained for wound treatment [2, 3]. After the war, studies revealed that tacrine was an effective acetylcholinesterase (AChE) inhibitor and could be used for Alzheimer's disease (AD). Tacrine crosses the blood-brain barrier easily and effectively inhibits central AChE [4]. Its tricyclic structure is

the major factor in AChE inhibition [5]. Its use for AD started in 1984, and its results was first reported in 1986 [6]. It is the first drug for AD treatment receiving FDA approval [7]. As determined by crystallographic studies, tacrine binds directly and selectively to the active site of AchE without interacting with any other site [8]. Since tacrine displays unusual interaction properties, many computational studies were also reported on tacrine [9–11].

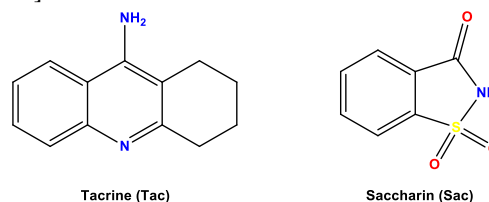


Fig. 1. 2D representation of tacrine (Tac) and saccharin (Sac) molecules

¹ Corresponding Author

e-mail: nursel.acar@ege.edu.tr

Another such molecule is saccharin (1,2-benzisothiazol-3(2H)-one-1,1-dioxide, Fig. 1), a commercial artificial sweetener [12]. Artificial sweeteners, including saccharin, are sugar replacements for many diseases like diabetes and obesity. However, use of these substitutes can result in severe health problems including bladder cancer, heart failure, and brain tumors as well as psychological and mental disorders [13–18]. Recently, many producers started to replace saccharin with alternative sweeteners due to speculations on its carcinogenic effects [12]. Although most of the studies on saccharin are experimental, molecular modeling studies were also reported on saccharin and its anion [12, 19–22].

Amidines have amide and imine functional groups and are referred as nitrogen analogues of

carboxylic acids [23]. An amino group replaces the hydroxyl moiety and an azomethine double bond replaces the carbonyl group. Structurally, they are carboxylic acid imidates [24, 25] and their pK_a values are within the range of 5–12 [26].

If they are protonated, they behave as strong organic bases caused by the charge delocalization on two nitrogens. The amidine structure also attract attention as it can establish specific interactions with proteins mainly through bidentate hydrogen bonds, and the amidino group can modulate this recognition process [27]. In the literature, many bioactive amidine based inhibitors are reported for three enzyme families: the NOS, the dimethylarginine dimethylaminohydrolase (DDAH) and the peptidylarginine deiminase (PAD) [28].

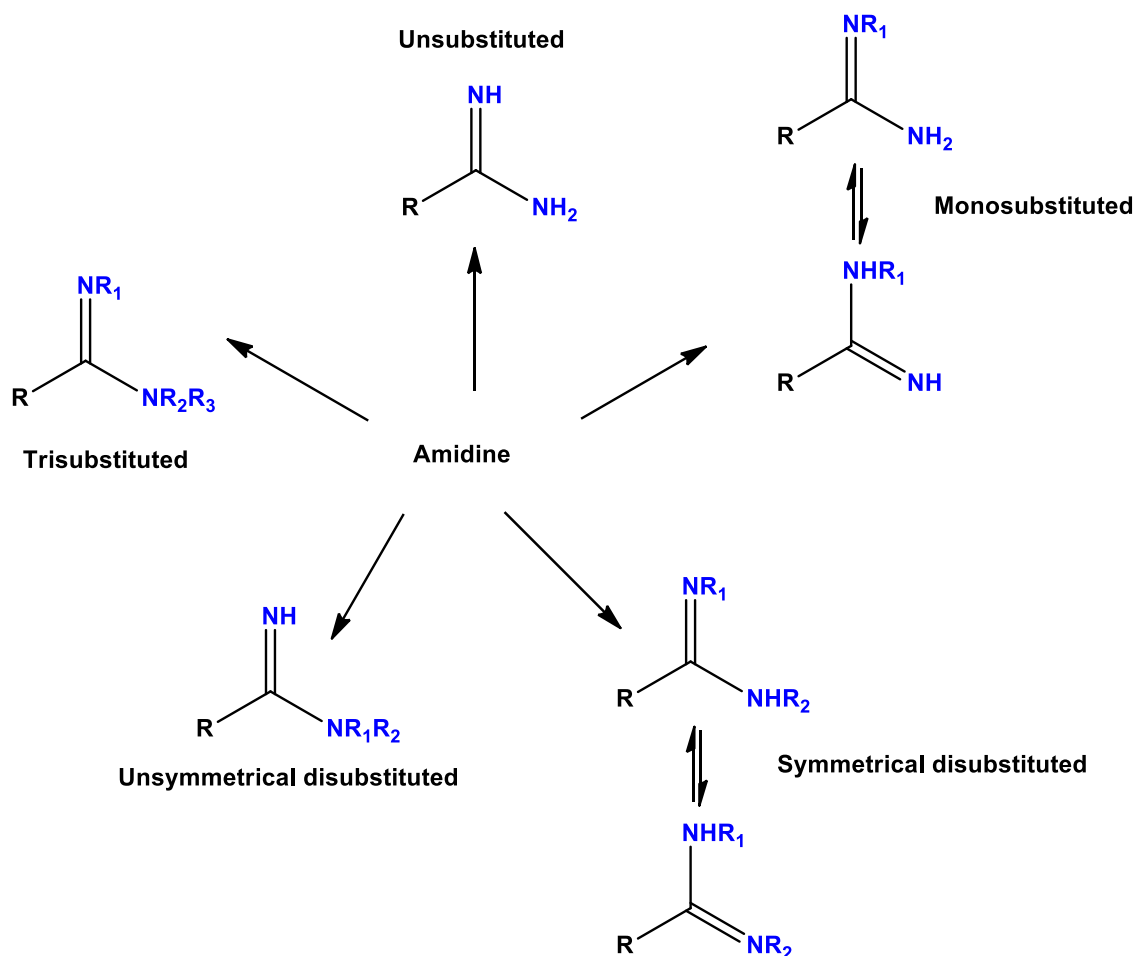


Fig. 2. Five amidine classes described by Shriner and Neumann [29].

A general classification of amidines is given by Shriner and Neumann depending on the substitution characteristics of nitrogen atoms: (i) unsubstituted, (ii) monosubstituted, (iii) symmetrical disubstituted, (iv) unsymmetrical disubstituted, (v) trisubstituted [29]. General structure of these amidine types are displayed in Fig. 2.

Major components of DNA, the nucleobases are also amidines [30]. They are used in organic synthesis [31], and attract attention for their unique properties like prototropy [30] and superbasicity [32]. Amidine derivatives are also used as antiparasitics [33], antitumor drugs [34], purification agents [35], nucleophilic catalysts [36], fungicides [37], and polymeric adhesives [38]. A recent study revealed that amidine conjugation may also play a significant role on electronic structures by stabilizing unstable intermediates and enabling researchers to isolate these compounds [39]. Some additional properties are reported in a recent review [40].

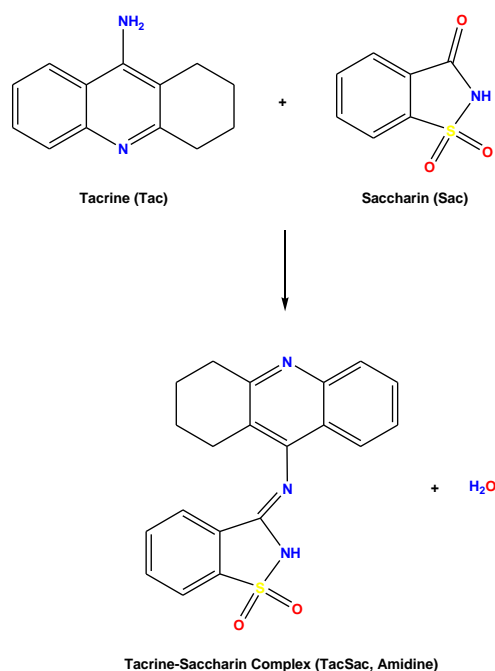


Fig. 3. Schematic representation for the formation reaction of Tacrine-Saccharin complex (TacSac)

There are many studies reported on tacrine and saccharin; but, neither experimental nor computational studies are reported on the tacrine-saccharin complex formed by the reaction of tacrine

and saccharin to form an amidine (TacSac, Fig. 3) except our recent computational study [41]. We investigated the spectroscopic properties of TacSac using density functional theory (DFT) and time-dependent density functional theory (TDDFT) with different functionals. The computational spectra were in good agreement with experimental results but there were some discrepancies about the structures with different solvent approaches. In current study, it is our aim to clarify those discrepancies by repeating the calculations at a higher ab initio level including electron correlation.

2. Computational Method

The initial geometries obtained from the conformational research in our previous work [41] were used for Tac, Sac and TacSac. The structures of investigated systems were visualized by Gaussview 5.0.9 [42]. Geometry optimizations and frequency calculations were performed with Gaussian 09 Revision-C.01 [43]. Second order Møller-Plesset perturbation (MP2) method [44, 45] was used to optimize all possible conformers of the investigated structures in both media. Pople type 6-311++G(d,p) basis set was used in all calculations [46]. Frequency calculations followed geometry optimizations and all calculated frequencies were positive. The most stable conformer for each system was used in further calculations.

To obtain the computational UV-Vis spectra, excited state calculations on ground state structures were carried out with CIS method [47] and Time-Dependent Density Functional Theory (TDDFT) using B3LYP (Becke-style three-parameter functional with Lee-Yang-Parr exchange-correlation) [48, 49] and CAM-B3LYP (Coulomb-attenuating method for B3LYP) [50] functionals using the same basis set. The latter includes long range corrections to B3LYP method. For each investigated system, the first 100 singlet excited states were taken into account.

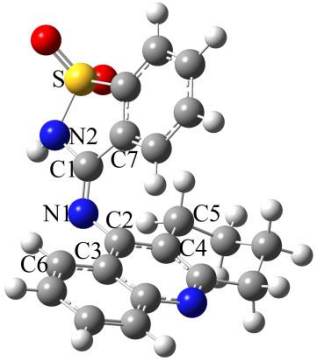
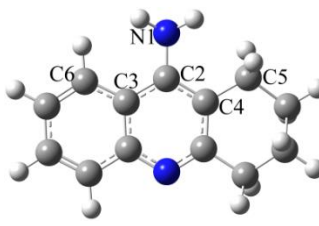
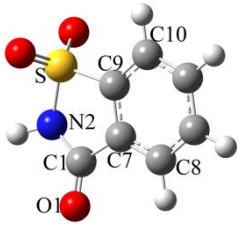
The polarizable continuum model (PCM) [51, 52] was used with default options in Gaussian 09 to evaluate the solvent effect. Calculations were repeated with the SMD (solvation model based on density) approximation [53] to observe the contributions of nonelectrostatic solute-solvent interactions. Atomic Polar Tensor (APT) approach was used for charge analysis [54].

3. Results and discussion

The results are discussed in three sections. The first part reports the calculated geometries and energies of investigated systems in gas phase and in

solution. Second part focuses on UV-Vis spectra and electronic transitions and the third part summarizes the results on charge analysis.

Table 1. Optimized geometries and some selected structural parameters for the investigated systems in gas phase and in solution at MP2/6-311++G(d,p)

	TacSac			Tac			Sac		
									
Bond Lengths	GAS	H2O	H2O (SMD)	GAS	H2O	H2O (SMD)	GAS	H2O	H2O (SMD)
N1C2	1.411	1.411	1.413	1.396	1.390	1.389	-	-	-
C2C3	1.419	1.419	1.418	1.427	1.429	1.429	-	-	-
C2C4	1.395	1.395	1.394	1.396	1.398	1.398	-	-	-
N1C1	1.285	1.285	1.285	-	-	-	-	-	-
O1C1	-	-	-	-	-	-	-	1.216	1.219
C1N2	1.405	1.407	1.410	-	-	-	1.399	1.396	1.395
C1C7	1.485	1.482	1.480	-	-	-	1.492	1.489	1.486
Bond Angles									
C1N1C2	116.50	117.20	116.45	-	-	-	-	-	-
N1C1N2	120.27	119.89	119.64	-	-	-	-	-	-
O1C1N2	-	-	-	-	-	-	124.99	124.55	124.07
N1C2C3	119.48	119.22	119.46	120.17	120.29	120.53	-	-	-
N1C2C4	120.13	120.23	119.89	120.62	120.61	120.45	-	-	-
N2C1C7	109.05	109.20	109.42	-	-	-	108.12	108.42	108.87
N2SC9	91.02	91.73	92.41	-	-	-	91.04	91.63	92.16
Dihedral Angles									
C1N1C2C3	108.14	108.91	107.44	-	-	-	-	-	-
N2C1N1C2	175.27	175.32	175.09	-	-	-	-	-	-
N1C2C3C6	-3.15	-4.46	-4.84	-3.18	-3.94	-3.96	-	-	-
N1C2C4C5	2.04	3.08	3.50	2.39	2.77	2.54	-	-	-
N2C1C7C8	160.78	162.05	163.13	-	-	-	172.10	172.99	172.89
N2SC9C10	-167.61	-169.02	-169.94	-	-	-	173.26	174.09	174.17

3.1. Optimized Structures

MP2/6-311++G(d,p) level was used to investigate the structures of Tacrine (Tac), Saccharin (Sac) and their complex (TacSac). The

optimized structures and some selected structural parameters are given in Table 1. A simplified numbering system is used to follow the parameters easily and may vary for each studied system.

As seen from Table 1, there are no significant changes in the geometries of investigated systems in different media. However, the geometry of TacSac presents significant differences compared to its parent compounds Tac and Sac. The N1C2 (~0.015 Å) and C1N2 (~0.010 Å) bond lengths increased in contrast to C2C3 (~0.010 Å) and C1C7 (~0.010 Å) which decreased in TacSac. Interestingly, C2C4 bond length change is negligible. This may be explained by the fact that C2C4 bond lies on the aliphatic side of the Tac and affected least by the changes in the resonance structure of the aromatic moiety. Similar changes are observed for bond angles, too. N1C2C3 decreases approximately 1° compared to Tac whereas N2C1C7 increases by the same amount compared to Sac. N1C2C4 and N2SC9 are almost identical without any significant changes. The most significant changes are observed for dihedral angles as expected. After the two cyclic molecules are covalently bonded through C-N double bond, steric repulsions occur due to the close contacts between

two cyclic systems. As seen by the changes for N1C2C3C6, N1C2C4C5, N2C1C7C8 and N2SC9C10 dihedrals, both cyclic molecules are distorted from their initial geometries in TacSac due to steric repulsions. The deviations are larger with respect to Sac which go up to 10° whereas it is much smaller (around 1°) compared to Tac.

The results revealed that the geometry is only slightly affected by the presence of a polar solvent (H₂O). Since the IEF-PCM model is an implicit model, it only calculates the electrostatic interactions and it is not possible to investigate specific interactions (i.e. hydrogen bonding) between solute and solvent molecules. Interestingly, inclusion of nonelectrostatic terms to IEF-PCM by SMD approach does not show any significant changes in the geometries in contrast to our former results [41]. It may be concluded that steric factors dominate over all other possible factors effecting geometries for the investigated systems.

Table 2. Calculated total electronic energies with zero-point energy corrections ($E_{TOT}(ZPE)$, Hartree), dipole moments (μ , Debye), sum of total electronic energy, ZPE and Gibbs free energy (ΔG , Hartree), complexation energies (E_C , kcal/mol) and changes in Gibbs free energy ($\Delta\Delta G$, kcal/mol) for the investigated systems calculated at MP2/6-311++G(d,p) in gas phase and in solution (in H₂O).

Gas	$E_{TOT}(ZPE)$ (Hartree)	μ (Debye)	ΔG (Hartree)	E_C^a (kcal/mol)	$\Delta\Delta G^b$ (kcal/mol)
Tacrine	-611.4375992	3.30	-611.4751130	-5.05	-1.84
Saccharin	-946.3721482	5.15	-946.4074900		
TacSac	-1481.5645700	4.19	-1481.6146770		
H ₂ O	-76.2532253	2.26	-76.2708660		
H₂O					
Tacrine	-611.4479910	4.99	-611.4855070	-5.15	-1.90
Saccharin	-946.3874805	6.55	-946.4228630		
TacSac	-1481.5823220	5.47	-1481.6323980		
H ₂ O	-76.2613553	2.51	-76.2790020		
H₂O (SMD)					
Tacrine	-611.4532624	5.51	-611.4908310	-8.62	-5.42
Saccharin	-946.3926688	7.23	-946.4279150		
TacSac	-1481.5925607	6.01	-1481.6426200		
H ₂ O	-76.2671048	2.72	-76.2847570		

$$^a\Delta E_C = (E_{TacSac} + E_{H_2O}) - (E_{Tac} + E_{Sac})$$

$$^b\Delta\Delta G = (\Delta G_{TacSac} + \Delta G_{H_2O}) - (\Delta G_{Tac} + \Delta G_{Sac})$$

Table 2 summarizes some calculated properties including total electronic energies, Gibbs free energy differences and dipole moments according to the reaction given in Fig. 3. In our former DFT study [41], our results indicate that formation of the TacSac complex requires energy (E_C values vary between +5 to +12 kcal/mol) and is a nonspontaneous endergonic process with $\Delta\Delta G$ values around +10 kcal/mol. However, in current study, MP2 results revealed a quite opposite tendency. As seen in Table 2, formation of TacSac is a spontaneous exergonic process in all media with negative $\Delta\Delta G$ values and E_C values vary between -5 to 8 kcal/mol. Depending on new MP2 results, it may be concluded that the formation

reaction for TacSac is much easier than formerly predicted. Another important outcome from Table 2 is the energy values calculated with SMD approximation. Although nonelectrostatic interactions do not play major roles in geometries of investigated systems, their contributions to the electronic and free energies are significant. By inclusion of SMD terms both E_C and $\Delta\Delta G$ values become more negative by approximately 3.50 kcal/mol. This observation is similar to our former DFT results.

3.2. UV-Vis Spectra and Electronic Transitions

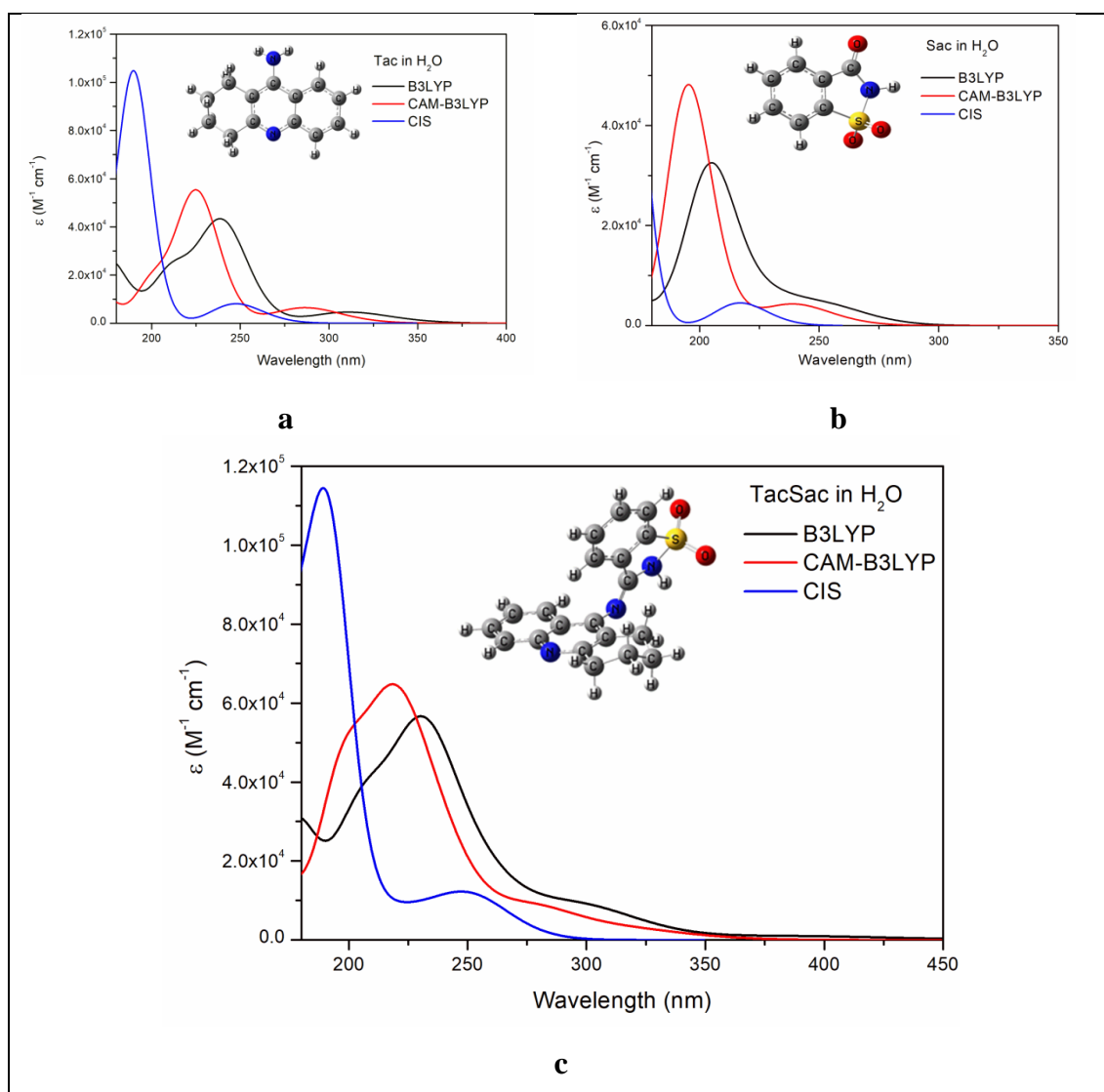


Fig. 4. Calculated UV-Vis spectra of a) Tac, b) Sac and, c) TacSac in H₂O with different methods using 6-311++G(d,p) basis set

In our previous study, we performed TD-DFT calculations to obtain UV-Vis spectra with different functionals on ground state geometries obtained at B3LYP/6-311++G(d,p) level using the first 40 singlet states [41]. The experimental and computational results were in good agreement but because of the discrepancies in the optimized TacSac geometries, the calculations were repeated with ground state geometries obtained at MP2/6-311++G(d,p) level. In order to compare results, the CIS method and B3LYP and CAM-B3LYP functionals together with 6-311++G(d,p) basis set were used to obtain first 100 singlet states.

Fig. 4 displays the calculated UV-Vis spectra of investigated compounds in H₂O with different methods. Comparison of the UV-Vis spectra with available experimental data reported in [41], B3LYP/6-311++G(d,p) level is determined to have the best correlation to the experimental results. The

following discussion is based on B3LYP/6-311++G(d,p) results unless otherwise stated.

Electronic transitions and related properties calculated at B3LYP/6-311++G(d,p) level for Tac, Sac and TacSac are given in Tables 3, 4 and 5, respectively. As seen in Table 3 and Fig 4, Tac has a peak at 312 nm. This peak corresponds to local excitation of Tac (LE1) at S₁ transition. There is also an intramolecular charge transfer (ICT) from NH₂ substituent towards the ring system of Tac observed at 247 nm with an n → π* transition character. This transition is also observed at 289 nm from H → L+1 with a very small oscillator strength. The molecular orbitals contributing to the electronic transitions observed for Tac, Sac and TacSac are given in Fig. S1.

Sac has a peak at 273 nm (Fig 4, Table 4) which corresponds to its local excitation (LE2). This observation is also supported by the results calculated for TacSac in the further discussion.

Table 3. Electronic transitions (λ_{ex}) correlated to vertical excitation energies (ΔE), transition dipole moments (μ_{tr}), oscillator strengths (f), excitation character, molecular orbitals with their % contributions in water calculated at B3LYP/6-311++G(d,p) level for Tac

state	ΔE (eV)	λ_{ex} (nm)	μ_{tr} (D)	f	Character ^a	Predominant Transitions	%
S ₁	3.97	311.6	1.1441	0.1115	LE1	H→L	69
S ₂	4.29	288.9	0.0365	0.0038	ICT,LE1	H-1→L	50
					ICT,LE1	H→L+1	49
S ₃	4.56	271.6	0.0125	0.0014	LE1	H-2→L	69
S ₄	5.01	247.3	0.4847	0.0595	ICT	H→L+2	66
S ₅	5.14	241.0	1.8928	0.2385	LE1	H-3→L	51
					ICT,LE1	H-1→L	29
					ICT,LE1	H→L+1	39
S ₆	5.17	239.7	5.4946	0.6964	LE1	H-3→L	36
					ICT,LE1	H-1→L	34
S ₇	5.38	230.3	0.2568	0.0339	ICT,LE1	H-2→L+1	68
					ICT	H→L+3	53
S ₈	5.46	227.2	0.0668	0.0089	ICT	H→L+4	44
					LE1	H→L+4	51
S ₉	5.48	226.1	0.1729	0.0232	ICT	H→L+3	43
					LE1	H→L+5	62
S ₁₀	5.61	221.1	0.0568	0.0078	LE1	H→L+5	62
S ₁₁	5.76	215.4	1.4070	0.1985	ICT,LE1	H-1→L+1	58

^aLE1 = local excitation of tacrine; ICT = intramolecular charge-transfer

Table 4. Electronic transitions (λ_{ex}) corresponding to vertical excitation energies (ΔE), transition dipole moments (μ_{tr}), oscillator strengths (f), excitation character, molecular orbitals and their % contributions in water calculated at B3LYP/6-311++G(d,p) level for Sac

State	ΔE (eV)	λ_{ex} (nm)	μ_{tr} (D)	f	Character ^a	Predominant Transitions	%
S ₁	4.54	273.0	0.0162	0.0018	LE2	H-2→L	65
S ₂	4.74	261.7	0.2580	0.0299	ICT,LE2	H→L	58
					LE2	H-1→L	27
S ₃	4.94	250.9	0.5353	0.0648	LE2	H-1→L	52
					ICT,LE2	H→L	30
S ₄	5.40	229.8	0.9073	0.1200	ICT2	H-3→L	60
					LE2	H-2→L	23
S ₅	5.82	212.9	0.1859	0.0265	ICT2,LE2	H-2→L+1	64
S ₆	5.97	207.5	3.0939	0.4528	ICT2	H-1→L+1	41
					LE2	H→L+1	34
S ₇	6.03	205.5	0.0779	0.0115	LE2	H-4→L	67
S ₈	6.07	204.2	0.0761	0.0113	ICT2	H-3→L+1	65
S ₉	6.15	201.4	2.1235	0.3203	LE2	H→L+1	51
					ICT2	H-1→L+1	36

^aLE2 = local excitation of saccharin; ICT = intramolecular charge-transfer

Table 5. Electronic transitions (λ_{ex}) correlated to vertical excitation energies (ΔE), transition dipole moments (μ_{tr}), oscillator strengths (f), excitation character, molecular orbitals and their % contributions in water calculated at B3LYP/6-311++G(d,p) level for TacSac

state	ΔE (eV)	λ_{ex} (nm)	μ_{tr} (D)	f	Character ^a	Predominant Transitions	%
S ₁	3.16	391.6	0.2934	0.0228	CT1	H→L	69
S ₂	3.80	325.9	0.2010	0.0187	CT1	H-1→L	70
S ₃	4.08	303.7	0.7556	0.0756	CT1	H→L+2	55
					LE1,CT1	H→L+1	40
S ₄	4.11	301.7	0.5359	0.0540	LE1,CT	H→L+1	50
					CT1	H→L+2	37
S ₅	4.14	299.8	0.1309	0.0133	CT1	H-2→L	61
					LE1,CT1	H→L+1	22
S ₆	4.35	285.1	0.4522	0.0482	LE1,CT1	H-1→L+1	52
					LE1	H→L+3	38
S ₇	4.40	281.6	0.2739	0.0296	LE2,CT1	H-3→L	55
					LE2,CT1	H-4→L	27
S ₈	4.58	270.7	0.1397	0.0157	LE1,CT1	H-2→L+1	60
					CT1	H-2→L	24
S ₉	4.69	264.1	0.1391	0.0160	CT1	H-1→L+2	42
					LE2	H-5→L	41
S ₁₀	4.70	263.7	0.1911	0.0220	CT1	H-1→L+2	56
					LE2	H-5→L	34
S ₁₁	4.83	256.4	1.9934	0.2361	LE2,CT1	H-4→L	48
					LE2	H-5→L	29
S ₁₂	4.94	250.9	0.4617	0.0559	LE2	H-6→L	63

^aLE1 = local excitation of tacrine; LE2 = local excitation of saccharin; CT1 = charge-transfer from tacrine to saccharin

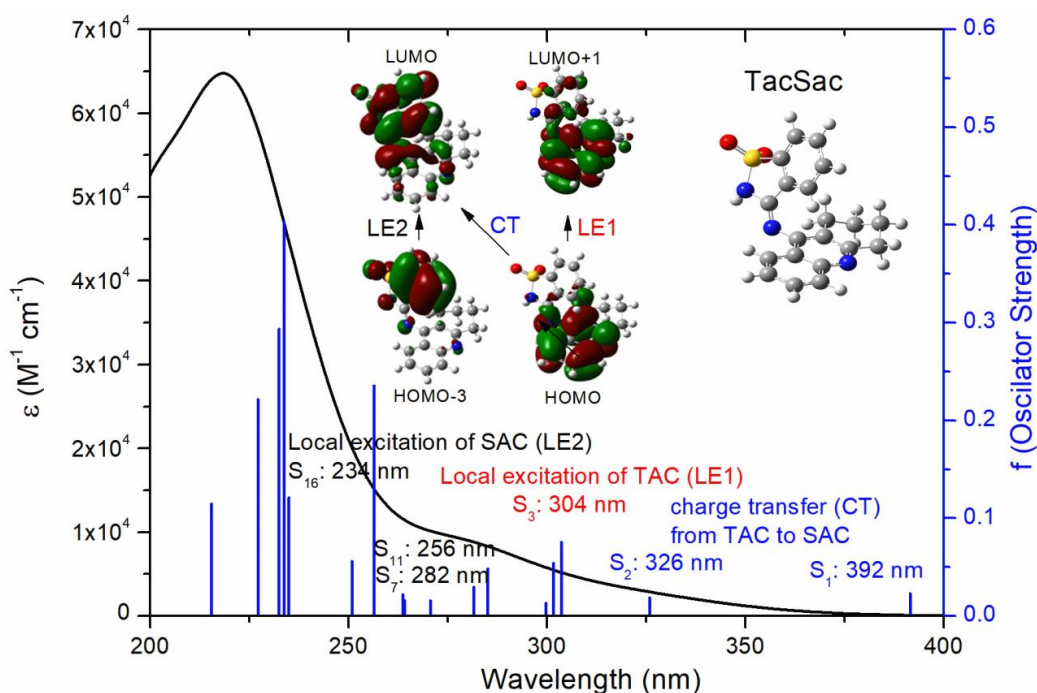


Fig. 5. Calculated UV-Vis spectrum of TacSac in H₂O at B3LYP/6-311++G(d,p) including all major transitions and corresponding molecular orbitals.

TacSac displays additional characteristics compared to its parent compounds (Fig 4, Table 5). The S₁ electronic transition corresponds to a charge transfer from Tac to Sac (CT1) at 392 nm. LE1 of Tac shows itself at 304 nm with a 8 nm shift in TacSac. LE2 of Sac appears at 282 nm but it has a larger oscillator strength at 256 nm. Calculated UV-Vis spectrum of TacSac in H₂O including electronic transitions, their corresponding molecular orbitals, extinction coefficients, and oscillator strengths is shown in detail in Fig. 5.

3.3. Charge Analysis

In order to understand the changes in charge distribution of the systems upon formation of TacSac, charges obtained from Atomic Polar Tensors (APT) approach were calculated (Table 6).

As seen in Table 6, the charges on the atoms increased in solution significantly in all studied systems except C_{C-NH₂} of Tac which is neutral in all media. In all studied systems, the negative charges are located around N containing moieties. The charges on S are almost similar in Sac and TacSac as S is not affected from the reaction being far from the reaction site. Along with S atom, C atoms bonded to N containing moieties carry positive

charges due to electron distribution caused by these moieties. It is observed that this charge distribution became more significant in a polar solvent medium like H₂O. Charges of all atoms for Tac, Sac and TacSac are tabulated in supplementary information (Tables S2 and S3) and are also given in bar representation (Figs S2-S4).

APT charge analysis reveal that charge of the N atom in the ring decreases in TacSac compared to Tac (Tac: -0.683, TacSac:-0.538 in water) which may also reduce the transition dipole moment in electronic transitions. The calculated transition dipole moments for S₁ electronic transition of Tac and TacSac are 1.1441 D and 0.2934 D, respectively. This observation may explain the first electronic excitation peak (S₁) magnitudes for Tac (strong, f=0.115) and TacSac (weak, f=0.0228) as seen in Table 3 and Table 5. This transition has charge transfer character for TacSac; thus, it is not observed in the experimental UV-Vis spectrum due to its very small oscillator strength. Another important factor is the presence of highly positively charged S atom. Although the negative charge on N atom decreases in TacSac, S atom keeps its positive charge and may enhance charge transfer from Tac to Sac moiety.

Table 6. APT atomic charges for selected atoms of Tac, Sac and TacSac calculated in gas phase and in H₂O at MP2/6-311++G(d,p) level.

Compound	Atom	Gas	H ₂ O	H ₂ O (SMD)
Tacrine	N _{NH2}	-0.654	-0.984	-1.093
	C _{C-NH2}	0.036	0.061	0.058
	N	-0.460	-0.683	-0.747
Saccharin	C _{C=O}	1.145	1.682	1.885
	N _{NH}	-0.992	-1.397	-1.507
	S	2.185	3.101	3.298
TacSac	C _{C=N}	0.408	0.598	0.611
	N _{C=N}	-0.726	-1.058	-1.088
	C _{C=N}	0.898	1.307	1.349
	N _{NH}	-0.996	-1.403	-1.115
	N	-0.375	-0.538	-0.572
	S	2.177	3.168	3.330

4. Conclusion

MP2/6-311++G(d,p) level was used to investigate structure, UV-Vis spectra and charge distribution of the amidine (TacSac) formed by reaction of tacrine and saccharin. Based on the former data, this level was chosen to shed light on the structural discrepancies observed with DFT. Electronic transitions were determined using CIS and TD-DFT approaches with the same basis set. The calculations were repeated in solution using polarizable continuum model (PCM). SMD (solvation model based on density) approach was also used to observe the effects of nonelectrostatic factors.

Similar geometries for TacSac was obtained in gas phase and in H₂O both with PCM and SMD models in contrast to DFT results. Since the discrepancy was observed in PCM calculations in DFT, it may be concluded that the electrostatic interactions were overestimated in DFT-PCM calculations causing significant deviations in the geometry.

The results also revealed that the formed amidine is stable and its formation reaction may not be reversible. This conclusion is also significantly different than our former study as DFT results showed that the formation reaction of TacSac between tacrine and saccharin has highly positive complexation energy values and free energy differences.

In addition to calculations at CIS/6-311++G(d,p) level for excited state properties, TDDFT calculations were performed at B3LYP/6-

311++G(d,p) and CAM-B3LYP/6-311++G(d,p) levels. B3LYP results were calculated to agree better to the experimental UV-Vis spectra of Tac and Sac. TacSac has a peak at a higher wavelength enabling S₀→S₁ transition to occur with a lower energy. S₀→S₁ transition corresponds to full charge transfer (CT1) between the HOMO and LUMO orbitals of TacSac in H₂O at 392 nm.

The MP2 results indicate that the TacSac system can be easily synthesized with a condensation reaction, and the amidine product is a potential candidate for photochemical charge-transfer systems.

Acknowledgments

Some of the calculations were performed on TUBITAK-ULAKBIM TRUBA resources.

Appendix A. Supplementary Material

Supplementary material to this article can be found online at <https://doi.org/10.33435/tcandtc.486573>.

References

- [1] S. E. Freeman, R. M. Dawson, Tacrine: a pharmacological review, *Prog Neurobiol* 36 (1991) 257–277.
- [2] V. Tumiatti, A. Minarini, M. L. Bolognesi, A. Milelli, M. Rosini, C. Melchiorre, Tacrine derivatives and Alzheimer's disease. *Curr Med Chem* 17 (2010) 1825–1838.

- [3] A. Alberti, The chemical and biological properties of acridines. *Sci Prog* 37 (1949) 418–434.
- [4] F. H. Shaw, G. A. Bentley, The pharmacology of some new anticholinesterases, *Aust J Exp Biol Med Sci* 31 (1953) 573–576.
- [5] P. N. Kaul, Enzyme inhibiting action of tetrahydroaminoacridine and its structural fragments, *J Pharm Pharmacol* 14 (1962) 243–248.
- [6] W. K. Summers, L. V. Majovski, G. M. Marsh, K. Tachiki, A. Kling, Oral tetrahydroaminoacridine in long-term treatment of senile dementia, *Alzheimer type*, *N Engl J Med* 315 (1986) 1241–1245.
- [7] W. K. Summers, Tacrine, and Alzheimer's treatments, *J Alzheimers Dis* 9 (2006) 439–445.
- [8] M. Harel, I. Schalk, L. Ehret-Sabatier, F. Bouet, M. Goeldner, C. Hirth, P. H. Axelsen, I. Silman, J. L. Sussman, Quaternary ligand binding to aromatic residues in the active-site gorge of acetylcholinesterase, *Proceedings of the National Academy of Sciences USA* 90 (1993) 9031–9035.
- [9] L. Pishkar, P. R. Jamaat, S. Makarem, Theoretical study of structure spectral properties of tacrine as Alzheimer drug, *J Phys Theor Chem IAU Iran* 12(1) (2015) 69–75
- [10] K. Y. Wong, A. G. Mercader, L. M. Saavedra, B. Honarparvar, G. P. Romanelli, P. R. Duchowicz, QSAR analysis on tacrine-related acetylcholinesterase inhibitors, *Journal of Biomedical Science* 21 (2014) 84.
- [11] É. C. M. Nascimento, J. B. L. Martins, M. L. dos Santos, R. Gargano, Theoretical study of classical acetylcholinesterase inhibitors, *Chemical Physics Letters* 458 (2008) 285–289.
- [12] M. A. R. Matos, M. S. Miranda, V. M. F. Morais, J. F. Liebman, Saccharin: a combined experimental and computational thermochemical investigation of a sweetener and sulfonamide, *Molecular Physics* 103(2–3) (2005) 221–228.
- [13] R. Kant, Sweet proteins-potential replacement for artificial low calorie sweeteners, *Nutrition Journal* 4 (2004) 5.
- [14] M. R. Weihrauch, V. Diehl, H. Bohlen, Artificial sweeteners-are they potentially carcinogenic?, *Med Klin (Munich)* 96 (2002) 670–675.
- [15] R. B. Kanarek, Does sucrose or aspartame cause hyperactivity in children?, *Nutr Rev* 52 (1994) 173–175.
- [16] S. Cohen, What's the truth about the health risks of sugar substitutes such as saccharin and aspartame?, *Health News* 7(1) (2001) 10.
- [17] L. O. Nabors, Saccharin and aspartame: are they safe to consume during pregnancy?, *The Journal of Reproductive Medicine* 33 (1988) 102.
- [18] A. Hagiwara, S. Fukushima, M. Kitaori, M. Shibata, N. Ito, Effects of three sweeteners on rat urinary bladder carcinogenesis initiated by N-butyl-N-(4-hydroxybutyl)-nitrosamine, *Gann* 75 (1984) 763–768.
- [19] A. Brizuela, E. Romano, A. Yurquina, S. Locatelli, S. A. Brandan, Experimental and theoretical vibrational investigation on the saccharinate ion in aqueous solution, *Spectrochimica Acta A* 95 (2012) 399–406.
- [20] V. D. Filimonov, E. A. Krasnokutskay, O. K. Poleshchuk, Yu A. Lesina, V. K. Chaikovskii, Electronic structures and reactivities of iodinating agents in the gas phase and in solutions: a density functional study, *Russ Chem B+* 55(8) (2006) 1328–1336.
- [21] M. M. Branda, N. J. Castellani, S. H. Tarulli, O. V. Quinzani, E. J. Baran, R. H. Contreras, DFTstudy of electronic structure of saccharin, thiosaccharin, and their respective ions: effects of metal coordination on thiosaccharinate electronic structure. *International Journal of Quantum Chemistry* 89 (2002) 525–534.
- [22] M. Remko, Theoretical study of molecular structure and gas phase acidity of some biologically active sulfonamides, *The Journal of Physical Chemistry A* 107 (2003) 720–725.
- [23] J. Y. Quek, T. P. Davis, A. B. Lowe, Amidine functionality as a stimulus-

- responsive building block, *Chemical Society Reviews* 42 (2013) 7326-7334.
- [24] T. Ishikawa, in *Superbases for Organic Synthesis: Guanidines, Amidines, Phosphazenes and Related Organocatalysts*, ed. T. Ishikawa, John Wiley & Sons, Ltd, 2009, pp. 1–6.
- [25] T. I. a. T. Kumamoto, in *Superbases for Organic Synthesis: Guanidines, Amidines, Phosphazenes and Related Organocatalysts*, ed. T. Ishikawa, JohnWiley & Sons, Ltd, 2009, pp. 49–86.
- [26] A. A. Aly, A. M. Nour-El-Din, *Functionality of amidines and amidrazones*, *ARKIVOC I* (2008) 153–194.
- [27] S. Maddaford, S. C. Annedi, J. Ramnauth, S. Rakhit, *Advancements in the development of nitric oxide synthase inhibitors*, *Annu. Rep. Med. Chem.* 44 (2009) 27-50.
- [28] C. Maccallini, M. Fantacuzzi, R. Amoroso, *Amidine-Based Bioactive Compounds for the Regulation of Arginine Metabolism*, *Mini Reviews in Medicinal Chemistry* 13 (2013) 1305-1310.
- [29] R. L. Shriner, F. W. Neumann, *The chemistry of the amidines*, *Chemical Reviews* 35 (1944) 351–425.
- [30] E. D. Raczynska, M. Makowski, M. Hallmann, B. Kamińska, *Geometric and energetic consequences of prototropy for adenine and its structural model—a review*, *RSC Advances* 5 (2015) 36587–36604.
- [31] P. S. Lobanov, D. V. Dar'in, *Acetamidines and acetamidoximes containing an electron-withdrawing group at the α -carbon atom: their use in the synthesis of nitrogen heterocycles*, *Chem Heterocycl Compd* 49(4) (2013) 507–528.
- [32] J. Nowicki, M. Muszyński, J-P. Mikkola, *Ionic liquids derived from organosuperbases: en route to superionic liquids*, *RSC Advances* 6 (2016) 9194–9208.
- [33] M. N. C. Soeiro, K. Werbovetz, D. W. Boykin, W. D. Wilson, M. Z. Wang, A. Hemphill, *Novel amidines and analogues as promising agents against intracellular parasites: a systematic review*, *Parasitology* 140 (2013) 929–951.
- [34] R. A. Michelin, P. Sgarbossa, S. Mazzega Sbovata, V. Gandin, C. Marzano, R. Bertani, *Chemistry and biological activity of platinum amidine complexes*, *ChemMedChem* 6 (2011) 1172–1183.
- [35] V. T. Mathad, P. V. Solanki, V. Pavankumar, S. B. Uppelli, G. G. Sarode, *A process for preparation of dabigatran etexilate mesylate and intermediates thereof*, *PCT Int. Appl.* (2015), WO 2015128875 A2 Sep 03, 2015.
- [36] J. E. Taylor, S. D. Bull, J. M. J. Williams, *Amidines, isothioureas, and guanidines as nucleophilic catalysts*, *Chemical Society Reviews* 41 (2012) 2109–2121.
- [37] J. W. Liebeschuetz, R. B. Katz, A. D. Duriatti, M. L. Arnold, *Rationally designed guanidine and amidine fungicides*, *Pestic Sci* 50 (1997) 258–274.
- [38] G. Wulff, R. Schönfeld, *Polymerizable amidines—adhesion mediators and binding sites for molecular imprinting*, *Adv Mater* 10(12) (1998) 957–959.
- [39] S. Erol Gunal, G. Sabuncu Gurses, S. Sag Erdem, I. Dogan, *Synthesis of stable tetrahedral intermediates (hemiaminals) and kinetics of their conversion to thiazol-2-imines*, *Tetrahedron* 72 (2016) 2122-2131.
- [40] G. Kantin, M. Krasavin, *N-arylation of amidines and guanidines: an update*, *Current Organic Chemistry* 20(13) (2016) 1370-1388.
- [41] N. Acar, C. Selçuki, E. Coşkun, *DFT and TDDFT investigation of the Schiff base formed by tacrine and saccharin*, *Journal of Molecular Modeling* 23 (2017) 17.
- [42] R. D. Dennington II, T. A. Keith, J. M. Millam, *GaussView 5.0.9*, Wallingford, CT, (2009)
- [43] M. J. Frisch, G. W. Trucks, H. B. Schlegel, G. E. Scuseria, M. A. Robb, J. R. Cheeseman, G. Scalmani, V. Barone, B. Mennucci, G. A. Petersson, H. Nakatsuji, M. Caricato, X. Li, H. P. Hratchian, A. F. Izmaylov, J. Bloino, G. Zheng, J. L. Sonnenberg, M. Hada, M. Ehara, K. Toyota, R. Fukuda, J. Hasegawa, M. Ishida, T. Nakajima, Y. Honda, O. Kitao, H. Nakai, T. Vreven, J. A. Montgomery Jr., J. E. Peralta, F. Ogliaro, M. Bearpark, J. J. Heyd, E.

- Brothers, K. N. Kudin, V. N. Staroverov, R. Kobayashi, J. Normand, K. Raghavachari, A. Rendell, J. C. Burant, S. S. Iyengar, J. Tomasi, M. Cossi, N. Rega, J. M. Millam, M. Klene, J. E. Knox, J. B. Cross, V. Bakken, C. Adamo, J. Jaramillo, R. Gomperts, R. E. Stratmann, O. Yazyev, A. J. Austin, R. Cammi, C. Pomelli, J. W. Ochterski, R. L. Martin, K. Morokuma, V. G. Zakrzewski, G. A. Voth, P. Salvador, J. J. Dannenberg, S. Dapprich, A. D. Daniels, Ö. Farkas, J. B. Foresman, J. V. Ortiz, J. Cioslowski, D. J. Fox, Gaussian 09, Revision C.01, Gaussian, Inc., Wallingford CT (2009).
- [44] M. J. Frisch, M. Head-Gordon, J. A. Pople, A direct MP2 gradient method, *Chemical Physics Letters* 166 (1990) 275-280.
- [45] M. Head-Gordon, J. A. Pople, M. J. Frisch, MP2 energy evaluation by direct methods, *Chemical Physics Letters* 153 (1988) 503-506.
- [46] W. J. Hehre, L. Radom, P. V. Schleyer, J. A. Pople, *Ab Initio Molecular Orbital Theory*, John Wiley & Sons, New York, USA, 1986, 576.
- [47] J. B. Foresman, M. Head-Gordon, J. A. Pople, and M. J. Frisch, Toward a Systematic Molecular Orbital Theory for Excited States, *The Journal of Physical Chemistry* 96 (1992) 135-149.
- [48] A. D. Becke, Density-functional thermochemistry. III. The role of exact exchange, *The Journal of Chemical Physics* 98 (1993) 5648-5652.
- [49] C. Lee, W. Yang, R. G. Parr, Development of the Colle-Salvetti correlation-energy formula into a functional of the electron density, *Physical Review B* 37 (1988) 785-789.
- [50] T. Yanai, D. Tew, N. Handy, A new hybrid exchange-correlation functional using the Coulomb-attenuating method (CAM-B3LYP), *Chemical Physics Letters* 393 (2004) 51–57.
- [51] J. Tomasi, B. Mennucci, E. Cancès, The IEF version of the PCM solvation method: an overview of a new method addressed to study molecular solutes at the QM ab initio level, *Journal of Molecular Structure THEOCHEM* 464 (1999) 211–226.
- [52] J. Tomasi, B. Mennucci, R. Cammi, Quantum mechanical continuum solvation models, *Chemical Reviews* 105 (2005) 2999–3093.
- [53] A. V. Marenich, C. J. Cramer, D. G. Truhlar, Universal solvation model based on solute electron density and on a continuum model of the solvent defined by the bulk dielectric constant and atomic surface tensions, *The Journal of Physical Chemistry B* 113 (2009) 6378–6396.
- [54] J. Cioslowski, A new population analysis based on atomic polar tensors, *Journal of American Chemical Society* 111(22) (1989) 8333–8336.